

SPWOOD: SPARSE PARTIAL WEAKLY-SUPERVISED ORIENTED OBJECT DETECTION

000
001
002
003
004
005 **Anonymous authors**
006 Paper under double-blind review
007
008
009
010

ABSTRACT

011 A consistent trend throughout the research of oriented object detection (OOD) has
012 been the pursuit of maintaining comparable performance with fewer and weaker
013 annotations. This is particularly crucial in the remote sensing domain, where
014 the dense object distribution and a wide variety of categories contribute to pro-
015hibitively high costs. Based on the supervision level, existing OOD algorithms
016 can be broadly grouped into fully supervised, semi-supervised, and weakly su-
017 pervised methods. Within the scope of this work, we further categorize them to
018 include sparsely supervised and partially weakly-supervised methods. To address
019 the challenges of large-scale labeling, we introduce the first Sparse Partial Weakly-
020 Supervised Oriented Object Detection (SPWOOD) framework, designed to effi-
021 ciently leverage only a few sparse weakly-labeled data and plenty of unlabeled
022 data. Our framework incorporates three key innovations: (1) We design a Sparse-
023 annotation-Orientation-and-Scale-aware Student (SOS-Student) model to separate
024 unlabeled objects from the background in a sparsely-labeled setting, and learn ori-
025 entation and scale information from orientation-agnostic or scale-agnostic weak
026 annotations. (2) We construct a novel Multi-level Pseudo-label Filtering (MPF)
027 strategy that leverages the distribution of model predictions, which is informed by
028 the model’s multi-layer predictions. (3) We propose a unique sparse partitioning
029 approach, ensuring equal treatment for each category. Extensive experiments on
030 the DOTA-v1.0/v1.5 and DIOR datasets show that SPWOOD framework achieves
031 a significant performance gain over traditional OOD methods mentioned above,
032 offering a highly cost-effective solution. Our code will be public soon.

1 INTRODUCTION

033 In the field of oriented object detection (OOD) task, early research is often supervised by rotated
034 bounding box (RBox) (Ding et al., 2019; Xie et al., 2021; Yang et al., 2019b; 2021), as shown in
035 Figure 1(a). However, the dense distribution and diverse nature of objects in the remote sensing
036 domain make it extremely difficult to obtain large-scale datasets with such detailed annotations.

037 To mitigate the reliance on fully annotated data, significant developments have been proposed, such
038 as semi-supervised oriented object detection (SOOD) (Hua et al., 2023; Liu et al., 2021; 2022; Wang
039 et al., 2025) and weakly supervised oriented object detection (WOOD) (Yang et al., 2023; Yu et al.,
040 2025a; Luo et al., 2024) shown in Figure 1(b-c). Semi-supervised methods utilize pseudo-labeling
041 strategies (Li et al., 2022a; Wang et al., 2023b) to learn angle and scale information from plenty of
042 unlabeled data. Weakly supervised methods use training data with less detailed labels, such as hori-
043 zontal bounding box (HBox) (Yu et al., 2023) or point (Yu et al., 2024; Ren et al., 2024; Zhang et al.,
044 2025). More recently, two notable subfields have emerged that integrate these approaches to further
045 the reduce annotation burdens: Partial weakly-supervised oriented object detection (PWOOD) (Liu
046 et al., 2025a) integrate the unlabeled and weakly annotated datasets. Sparsely supervised oriented
047 object detection (SAOD) (Suri et al., 2023; Rambhatla et al., 2022; Lu et al., 2024) leverage the
048 labeled datasets containing annotations for only a fraction of the objects in an image. As illustrated
049 in Figure 1(d-e), these methods alleviate the annotation dilemma further.

050 To further reduce annotation costs, we first propose a novel framework called Sparse Partial Weakly-
051 supervised Oriented Object Detection (SPWOOD). This framework effectively leverages sparsely
052 and weakly annotated data, along with unlabeled data. Inspired by the teacher-student paradigm

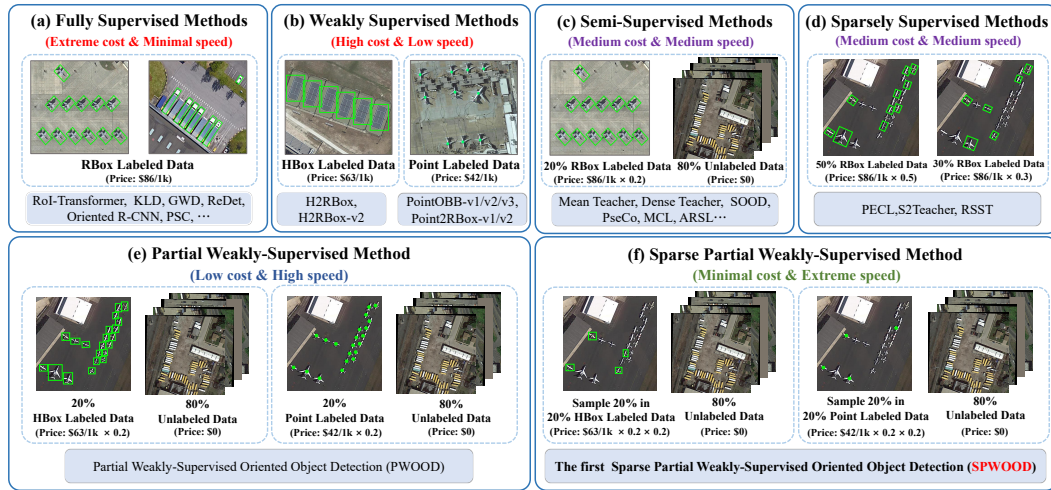


Figure 1: Current oriented object detection methods are predominantly classified into five categories. Compared to the aforementioned approaches, our proposed Sparse Partial Weakly-supervised Oriented Object Detection (SPWOOD) distinguished with minimal annotation requirements.

(Tervainen & Valpola, 2017), we leverage a small amount of sparsely and weakly annotated data for pre-training. Through this process, the student module learns the scale and angle information from weak annotations and acquires the ability to distinguish unlabeled object from background in the sparse annotation setting. As training progresses, the teacher module’s capabilities are continuously enhanced through Exponential Moving Average (EMA) mechanism. Upon entering the unsupervised learning stage, the teacher module generates pseudo-labels for unlabeled data. These pseudo-labels serve as a strong supervisory signal to train the student module, allowing it to learn from both the limited sparsely and weakly annotated data and the abundant unlabeled data. Consequently, pseudo-labels’ quality and the strategy used to filter them are crucial for model’s performance.

Traditional semi-supervised methods for pseudo-label selection typically depend on static thresholds (Liu et al., 2021; Wang et al., 2025), which often leads to performance that is sensitive across different training processes (Chen et al., 2022a; Wang et al., 2023b; 2022; Zhong et al., 2020). In contrast, PWOOD (Liu et al., 2025a) introduced a more robust approach by leveraging Gaussian Mixture Model (GMM) to cluster the teacher model’s predictions. While sparse-annotation methods, such as S²Teacher (Lin et al., 2025) and RSST (Liao et al., 2025), employed sophisticated techniques like top-k high-confidence proposal selection or a class-aware label assignment mechanism that leverages the distribution of class features. To better utilize the teacher module’s predictions in sparsely annotated setting, we design a Multi-level Pseudo-labels Filtering (MPF) mechanism. Considering the inconsistencies between different layers, we dynamically adjust the filtering threshold for each layer’s selection. This allows the model to adaptively generate more stable pseudo-labels that are better aligned with the teacher’s performance. Our approach improves the model’s ability to handle diverse and sparse scenarios, ultimately leading to more robust detection performance.

When creating sparse datasets, prior methods (Lu et al., 2024; Lin et al., 2025) follows what we term the Single Sparse Method, where annotations are processed on an image-by-image basis. A critical limitation of this technique is its inherent bias: when an image contains an annotation from a rare category, at least one annotation will be preserved simply. This disproportionately retains sparse categories and leads to a significant mismatch between the distribution of the processed data and the original dataset. To overcome this issue, we propose a novel approach called the Overall Sparse Method, treating all labeled annotations across the entire dataset as a single, unified group. This allows us to apply a consistent sampling ratio to each category, ensuring that every class is treated equally. As a result, our method effectively maintains the overall distribution of the original dataset. The contributions of this work are as follows:

- To our best knowledge, we introduce the first Sparse Partial Weakly-supervised Oriented Object Detection (SPWOOD) framework. This unified training pipeline is designed to robustly support various multi-format annotations (RBox, HBox, Point) or their combination as input under sparse partial annotation setting, thereby alleviating the significant burden of large-scale annotation.

- 108 • We construct a student model designed to acquire the crucial ability to perceive sparse annotation
109 environments and learn object orientation and scale information within the sparse partial weakly-
110 annotated scenarios. We term this model the SOS-Student model.
- 111 • The Multi-level Pseudo-labels Filtering (MPF) mechanism is designed to resolve the inconsistency
112 between traditional selection criteria and the model’s prediction confidence. By doing so, MPF
113 significantly enhances the robustness of the pseudo-label selection process for unlabeled data.
- 114 • We propose a fundamentally distinct sparse annotation approach for creating sparse-partial
115 datasets. Our SPWOOD framework has been rigorously trained and validated on the DOTA-
116 v1.0/v1.5 and [DIOR](#) sparse-partial settings. SPWOOD achieves performance highly comparable
117 to state-of-the-art Oriented Object Detection (OOD) algorithms.

119 2 RELATED WORK

120 2.1 SEMI-SUPERVISED ORIENTED OBJECT DETECTION

121 To effectively leverage abundant unlabeled data, the teacher-student framework has been widely
122 adopted in semi-supervised object detection (Li et al., 2022b; Liu et al., 2023; Nie et al., 2023; Sun
123 et al., 2021a). This method begins by training a student module on a limited set of fully labeled
124 data. A teacher module then acquires the ability to generate pseudo-labels for unlabeled data by
125 using an exponential moving average (EMA) of the student’s weights. These pseudo-labels subse-
126 quently guide the student’s training, creating a learning loop. For instance, MCL (Wang et al., 2025)
127 introduced a novel approach by introducing Gaussian Center Assignment for labeled data and Scale-
128 aware Label Assignment for unlabeled data. Besides, SOOD++ (Liang et al., 2024) treated remote
129 sensing images as global layouts, explicitly establishing a many-to-many relationship between sets
130 of pseudo-labels and predictions to enhance detection. However, despite their innovations, these
131 methods still rely on a substantial number of fully annotated RBox for their initial training.

132 2.2 WEAKLY SUPERVISED ORIENTED OBJECT DETECTION

133 Weakly supervised object detection algorithms (Bilen et al., 2015; Iqbal et al., 2021; Yang et al.,
134 2019a; Zhang et al., 2021; Zhu et al., 2023), as a significant breakthrough, offer a more efficient
135 alternative to fully supervised methods by leveraging weak annotation, such as HBox or point an-
136 notations. For HBox-supervised methods (Li et al., 2022c; Sun et al., 2021b; Tian et al., 2021;
137 Wang et al., 2024; Zhu et al., 2023), H2RBox (Yang et al., 2023) introduced a weakly supervised
138 branch and a self-supervised branch to learn both scale and orientation information. Building on
139 this, H2RBox-v2’s primary innovation lay in its symmetry-based self-supervised learning (Yu et al.,
140 2023), which directly derived crucial directional information from an object’s inherent symmetry.
141 For point-supervised methods, the main challenge is how to accurately learn object’s scale and angle
142 information. Recent studies have made significant progress in this area (Chen et al., 2021; 2022b;
143 He et al., 2023; Ying et al., 2023). P2RBox (Cao et al., 2023) and PointSAM (Liu et al., 2025b)
144 demonstrated remarkable performance by leveraging the zero-shot capabilities of the Segment Any-
145 thing Model (Kirillov et al., 2023). Additionally, PointOBB (Luo et al., 2024) and its subsequent
146 versions (Ren et al., 2024; Zhang et al., 2025) pushed the boundaries of point-supervised detection
147 by using instance learning to solve the scale problem and class probability map to acquire angle
148 information. More recently, Point2RBox (Yu et al., 2024) adopted a knowledge combination strat-
149 egy by introducing synthetically generated targets, offering prior scale imformation. Furthermore,
150 Point2RBoxv2 (Yu et al., 2025a) incorporated novel losses based on spatial layout constraints, which
151 ensure that predictions align more accurately with real-world object. Besides, Wholly-WOOD (Yu
152 et al., 2025b), a unified weakly supervised detector, accommodated multiple annotation formats in-
153 cluding Point/HBox/RBox or their combination as inputs. More specifically, PWOOD (Liu et al.,
154 2025a) merged the advantages of semi-supervised method and weakly supervised mthod to achieve
155 enhanced performance, all while substantially lowering annotation requirements.

156 2.3 SPARSELY SUPERVISED ORIENTED OBJECT DETECTION

157 In SAOD research filed, only a fraction of objects in an image are labeled, while the rest remains un-
158 labeled. Lack of complete annotations presents a major challenge, as the detector confuse unlabeled

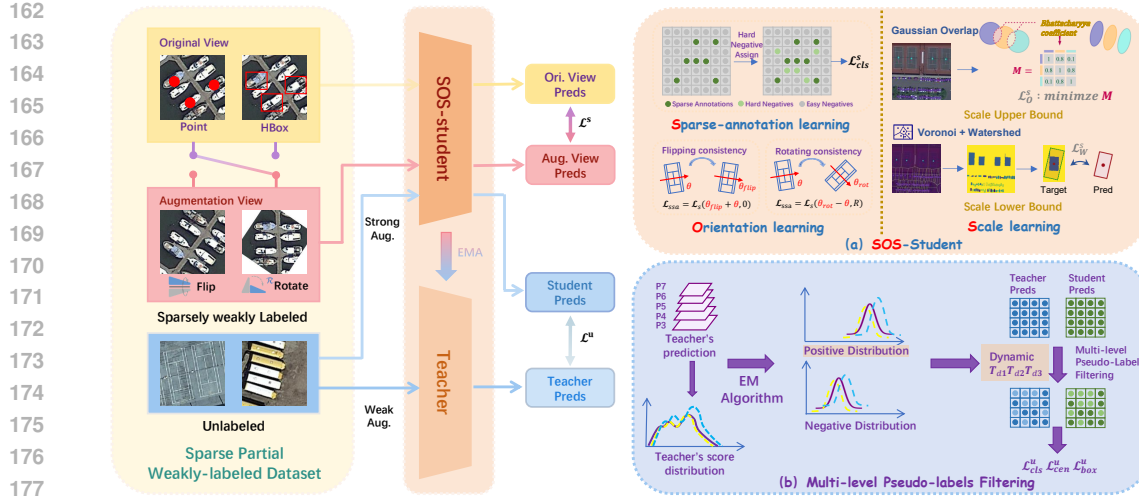


Figure 2: The illustration of the Sparse Partial Weakly-supervised Oriented Object Detection (SPWOOD). The Sparse-annotation-Orientation-and-Scale-aware Student (SOS-Student) identifies hard negatives and learn the scale and angle information from sparse weak annotation data. The Multi-level Pseudo-labels Filtering (MPF) mechanism acquires ability from student through EMA algorithm and selects high-quality pseudo-labels for student module’s training.

objects with the background, since both share the same “background” label. In the domain of 3D object detection, Coln (Xia et al., 2023) introduced a contrastive learning module to enhance feature discrimination and a feature-level pseudo-label mining framework to guide the training. HINTED (Xia et al., 2024) proposed a self-boosting teacher, leveraging instance-level information and updates pseudo-labels for labeled scenes to enhance learning effectiveness. When addressing similar challenges within the remote sensing domain, Co-mining (Wang et al., 2021) utilized a Siamese network to enhance multi-view learning, with two branches predicting pseudo-labels for each other via a co-generation module. Region-based approaches (Rambhatla et al., 2022) treated SAOD as a semi-supervised problem at the region level, focusing on identifying unlabeled regions that likely contain foreground objects. Calibrated Teacher (Wang et al., 2023a) introduced an online calibration mechanism to fit the true precision during training, improving pseudo-labels quality. PECL (Lu et al., 2024) offered a reinforcement learning-based selection strategy specifically tailored for pseudo-labels filtering. More recently, S²Teacher (Lin et al., 2025) proposed a clusterbased pseudo-label generation module to avoid erroneous guidance. RSST (Liao et al., 2025) designed a class-aware pseudo-labeling mechanism for both labeled and unlabeled data by integrating priors from large language model. In contrast to these methods, our approach innovatively integrates various supervised methods under minimal supervision cost.

3 METHOD

3.1 OVERVIEW

Given the setting consisting of abundant unlabeled data and a small amount of sparsely-weakly annotated data, we adopt a classic pseudo-labeling semi-supervised object detection (SSOD) framework. As shown in Figure 2, SPWOOD framework operates with two core branches: one for supervised learning and another for unsupervised learning. The supervised branch integrates sparse-annotation learning, scale learning, and orientation learning, which together form the SOS-Student module. The unsupervised branch leverages a Multi-level Pseudo-labels Filtering (MPF) mechanism to generate reliable supervisory signals used for student module’s subsequent training.

The training process unfolds in two distinct stages: (1) Burn-in Stage: The student module begins by training on a few sparse weak annotations from both original and augmented views. Concurrently, the learned weights of the SOS-Student module are mirrored onto the teacher module. (2) Self-training Stage: In this stage, a large volume of strongly-weakly-augmented unlabeled data is fed into the teacher module to generate pseudo-labels. The student module is then further optimized using these pseudo-labels. The teacher module is updated from the student’s module using an Exp-

ential Moving Average (EMA) (Tervainen & Valpola, 2017) approach, which ensures the teacher's parameters are more stable and reliable, leading to higher-quality pseudo-labels.

3.2 SOS-STUDENT

3.2.1 SPARSE ANNOTATION LEARNING

In the context of sparsely annotated data, a major challenge is effectively distinguishing unlabeled objects from background. Both are treated as negatives during training, leading to potential misguidance where unannotated objects are incorrectly penalized as background. Inspired by Focal Loss, designed to tackle the class imbalance problem by down-weighting the loss of easy-to-classify examples, we introduce a mechanism to differentiate between different types of negative samples by modulating their loss contribution (Liao et al., 2025). This strategy aims to balance the influence of false supervision and retain beneficial background cues. The loss function is formulated as follows:

$$\mathcal{L}_{cls}^s = \begin{cases} -\alpha_t(1 - p_t)^\gamma \log(p_t) & \text{for positive objects} \\ -(1 - \alpha_t)p_t^\gamma \log(1 - p_t) & \text{for negative objects with confidence } p_t \leq thr \\ -(1 - \alpha_t)p_t^\gamma \log(1 - p_t)\omega & \text{for negative objects with confidence } p_t > thr, \end{cases} \quad (1)$$

Our student classification loss, L_{cls}^s , aims to partition the prediction space into three distinct groups for effective learning under sparse supervision: Labeled Objects: Predictions with high confidence ($p_t > thr$) matching the ground truth (GT) labeled category. Background: Predictions with low confidence ($p_t \leq thr$) matching the GT background. Unlabeled Objects (Hard Negatives): Predictions with high confidence ($p_t > thr$) that are erroneously matched to the GT background. The base loss formulation incorporates standard components: p_t represents the confidence score from the student module; α_t serves as a balancing factor between positive and negative samples; and γ is the focusing parameter, designed to reduce the contribution of well-classified examples (inheriting the robustness of Focal Loss). For the critical third group (Unlabeled Objects), we introduce the adaptive factor ω . This factor strategically down-weights these potentially misleading false negatives. This novel strategy effectively inherits the robustness of Focal Loss while simultaneously providing a targeted solution for sparse annotation scenarios. By mitigating the detrimental effects of misleading false negatives, it leads to more accurate and robust model learning.

3.2.2 ORIENTATION LEARNING

To address the lack of orientation information in weakly-annotated data, like HBox annotations, we introduce a symmetry-aware learning approach (Yu et al., 2023) that comprehensively explores the properties of object symmetry. As depicted in Figure 2, each input image undergoes a random augmentation (either flipping or rotating) to create an augmented view. This view is then fed into the student module, which generates a pair of predicted angles. Since the input views have a clear relationship, the output angles are expected to follow the same relationship.

To ensure the SOS-Student effectively learns orientation information from the weakly annotated horizontal bounding boxes, we formulate an angle loss, \mathcal{L}_{Ang}^s

$$\mathcal{L}_{Ang}^s = \begin{cases} L_{Ang}^s(\theta_{flp} + \theta, 0) & \text{if augmentation is a flip} \\ L_{Ang}^s(\theta_{rot} - \theta, \mathcal{R}) & \text{if augmentation is a rotation by } \mathcal{R}. \end{cases} \quad (2)$$

The angle loss calculation depends on the specific image augmentation method model used, which can be either a vertical flip or a random rotation by an angle \mathcal{R} . The loss function L_{Ang}^s is a Smooth-L1 loss. Here, θ_{flip} , θ_{rot} , and θ represent the predicted angles of the flip-augmented image, the rotated-augmented image, and the original image, respectively.

3.2.3 SCALE LEARNING

Given that weaker annotations, such as point annotations, lack crucial scale and orientation information about the objects. To address this, we adopt spatial layout learning (Yu et al., 2025a) to learn the objects' scale information by determining both the upper and lower bounds.

270 Table 1: Comparison with state-of-the-art methods for the OOD task at different sparse-partial ratios.
 271 $\triangle 10\%$ and $\blacksquare 10\%$ denote the partial-ratio and sparse-ratio. RSST* represents our SAOD baseline
 272 and R:H:P means the annotations count ratio between RBox, HBox and Point.

			DOTA-v1.0 Dataset-Sparse-Partial					
Algorithm Types	Methods	Annotations	10% \triangle		20%		30%	
			10% \blacksquare	20%	10%	20%	10%	20%
Weakly Supervised	H2RBox-v2	HBox	30.6	30.8	38.5	42.7	43.9	49.2
	Point2RBox-v2	Point	9.4	9.8	14.2	23.1	15.1	27.0
Semi-Supervised	MCL	RBox	31.7	39.0	37.6	44.5	43.5	47.8
	PWOOD	RBox	38.0	46.2	46.2	51.9	48.7	55.2
Partial Weakly-Supervised	PWOOD	HBox	33.9	43.8	42.4	47.6	44.8	50.7
	PWOOD	Point	17.0	24.7	22.4	28.6	23.1	33.8
Sparsely Supervised	S ² Teacher	RBox	36.8	44.0	45.3	50.2	52.3	55.5
	RSST	RBox	43.4	47.2	42.5	52.3	53.0	56.6
	RSST*	RBox	42.4	45.5	41.7	51.0	53.2	56.5
Sparse Partial Weakly-Supervised	SPWOOD (ours)	RBox	48.5	54.0	54.9	57.8	54.9	60.3
		HBox	45.5	51.9	52.2	54.0	53.1	56.5
		Point	27.3	36.8	33.3	38.7	35.8	41.8
		R:H:P=1:1:1	42.4	48.2	46.1	53.0	50.8	54.8

291 For the upper bound of the object’s scale, we minimize the distance between different predicted
 292 oriented bounding boxes. We first model these boxes as two-dimensional Gaussian distributions and
 293 then use the Bhattacharyya distance (Yang et al., 2022) to calculate the distance between them. This
 294 allows us to derive the Gaussian overlap loss, \mathcal{L}_O^s , as follows:

$$\mathcal{L}_O^s = \frac{1}{N} \sum_{i \neq j} B(\mathcal{N}_i, \mathcal{N}_j), \quad (3)$$

298 where N donates the number of predicted rotated bounding boxes, \mathcal{N}_i and \mathcal{N}_j represent different
 299 Gaussian distribution, and B is the Bhattacharyya distance between them.

300 To determine the lower bound of the object’s scale, we introduce the Voronoi Watershed Loss. A
 301 Voronoi diagram (Aurenhammer, 1991) separates the entire image into individual regions, ensuring
 302 each region contains only one point annotation. These regions are then fed into a watershed algo-
 303 rithm (Vincent & Soille, 1991) to obtain a pixel-level classification based on pixel similarity. By
 304 rotating the output of the watershed algorithm to align with the direction of predicted rotated bound-
 305 ing boxes based on a single point, we can obtain the regression target of object’s width and height.
 306 The Voronoi watershed loss, \mathcal{L}_W , is then designed to regress the width and height of the objects:

$$\mathcal{L}_W^s = L_{GWD} \left(\left[\begin{matrix} w/2 & 0 \\ 0 & h/2 \end{matrix} \right]^2, \left[\begin{matrix} w_t/2 & 0 \\ 0 & h_t/2 \end{matrix} \right]^2 \right), \quad (4)$$

310 where L_{GWD} is Gaussian Wasserstein Distance Loss (Yang et al., 2022).

312 Finally, we incorporate class loss \mathcal{L}_{cls}^s , centerness loss \mathcal{L}_{cen}^s , and box loss \mathcal{L}_{box}^s . The total supervised
 313 loss, \mathcal{L}^s , for the SOS-Student model is given by:

$$\mathcal{L}^s = w_{cls} \mathcal{L}_{cls}^s + w_{cen} \mathcal{L}_{cen}^s + w_{box} \mathcal{L}_{box}^s + w_{Ang} \mathcal{L}_{Ang}^s + w_O \mathcal{L}_O^s + w_W \mathcal{L}_W^s, \quad (5)$$

316 where \mathcal{L}_{cls}^s , \mathcal{L}_{cen}^s , and \mathcal{L}_{box}^s represent the sparse annotation aware loss (as described in 3.2.1), the
 317 cross entropy loss and the IoU loss respectively. The weights w_{cls} , w_{cen} , w_{box} are set to 1, while
 318 (w_{Ang}, w_O, w_W) are set to (0.2, 10, 5) by default.

320 3.3 MULTI-LEVEL PSEUDO-LABELS FILTERING

322 The selection of pseudo-labels directly influences the performance of subsequent training. In SAOD
 323 setting, RSST (Liao et al., 2025) leverages classes’diversity and LLM’s assistance to select pseudo-
 324 labels, combining a fixed number of predictions per category and overall predictions. However,

324 Table 2: Comparison of mAP performance across different methods for the OOD task on DOTA-
 325 v1.5 test set under different sparse-partial ratios (RBox supervised).

327 Algorithm Types	328 Methods	329 10-10	330 10-20	331 20-10	332 20-20	333 30-10	334 30-20
329 Semi-Supervised	MCL	25.9	33.9	33.2	40.2	38.2	42.9
	PWOOD	33.9	38.1	40.9	45.9	45.1	49.2
331 Sparsely Supervised	S ² Teacher	33.8	37.2	41.1	45.7	45.7	46.2
	RSST	37.1	40.8	42.3	46.9	45.3	48.0
	RSST*	36.2	35.8	42.3	46.0	45.7	49.8
334 Sparse Partial 335 Weakly-Supervised	336 SPWOOD (ours)	43.2	47.9	49.0	52.1	51.3	53.1

337 ignoring the confidence variance throughout the training process of model makes the detector's per-
 338 formance sensitive. Furthermore, Feature Pyramid Networks (FPN) (Lin et al., 2017) is specialized
 339 for detecting objects at corresponding scales and the same object exhibits different confidence scores
 340 at different levels (*i.e.* P3, P4, P5, P6, P7), making modeling the entire prediction directly unreliable
 341 as Class-Agnostic PseudoLabel Filtering strategy (CPF) (Liu et al., 2025a).

342 To better utilize the information from the model's prediction and discover reliable pseudo-labels,
 343 we focus on the distribution of the teacher's predictions by introducing Multi-level Pseudo-labels
 344 Filtering. Based on a Gaussian Mixture Model (GMM) (Wang et al., 2023b; Zhao et al., 2019), we
 345 model the prediction confidence of each layer in the teacher module with the following equation:
 346

$$347 \quad \mathcal{P}^i(c^i) = w_p^i \mathcal{N}_p^i(\mu_p^i, (\sigma_p^i)^2) + w_n^i \mathcal{N}_n^i(\mu_n^i, (\sigma_n^i)^2), \quad (6)$$

349 where $\mathcal{P}^i(c^i)$ means the modeling of i -th level, such as P3, P4, P5, P6 and P7. $\mathcal{N}(\mu, \sigma^2)$ denotes
 350 gaussian distribution, while w_p , μ_p , σ_p and w_n , μ_n , σ_n represent the weight, mean and variance
 351 of positive and negative distributions, respectively. **The GMM is initialized by setting μ_p and μ_n to the maximum and minimum of the predicted scores, respectively. The variances (σ_p and σ_n) and weights (w_p and w_n) are all initially set to 1 and 0.5, respectively.** We then use Expectation-
 352 Maximization (EM) algorithm to solve for the posterior probability, \mathcal{P} , with the following equation:
 353

$$356 \quad \tau^i = \arg \max_{c^i} \mathcal{P}^i(c^i, \mu_p^i, (\sigma_p^i)^2), \quad (7)$$

359 where τ^i is then used to select pseudo-labels at the corresponding scale level. The selected pseudo-
 360 labels from each layer are subsequently used to guide the student module's training.

362 3.4 OVERALL LOSS

364 Our proposed SPWOOD framework contains two branches: one for the supervised loss \mathcal{L}^s and
 365 another for the unsupervised loss \mathcal{L}^u . The combination of these two losses constitutes the overall
 366 loss. The former one is detailed in dection 3.2.3. The latter one is defined as below:

$$368 \quad \mathcal{L}^u = \mathcal{L}_{cls}^u(\mathcal{T}^c, \mathcal{S}^c) + \mathcal{L}_{cen}^u(\mathcal{T}^{cen}, \mathcal{S}^{cen}) + \mathcal{L}_{box}^u(\mathcal{T}^{logit}, \mathcal{S}^{logit}), \quad (8)$$

369 where \mathcal{T} and \mathcal{S} represent the predictions of the teacher and student modules, respectively. These
 370 prediction include the confidence score (c), centerness (cen) and the margin from the point to the
 371 boundaries of the predicted boxes. The loss function \mathcal{L}_{cls}^u and \mathcal{L}_{cen}^u are binary cross-entropy losses,
 372 while \mathcal{L}_{box}^u is Smooth-L1 loss. The overall loss of SPWOOD framework is defined as:
 373

$$374 \quad \mathcal{L} = \mathcal{L}^s + \mathcal{L}^u. \quad (9)$$

376 Through these two complementary branches, the student learns from sparsely-weakly annotated
 377 data, enhancing the teacher's pseudo-labels filtering ability. In turn, the high-quality pseudo-labels
 selected by teacher further improve the student's learning, forming a positive feedback learning loop.

378 Table 3: Comparison of mAP performance across different methods for the OOD task on DIOR test
 379 set under different sparse-partial ratios (RBox supervised).

Algorithm Types	Methods	10-20	20-20	30-20
Semi-Supervised	MCL	30.8	33.1	35.8
	PWOOD	31.0	36.8	39.1
Sparsely Supervised	S ² Teacher	36.1	42.6	45.1
	RSST	40.7	44.8	46.1
	RSST*	38.8	43.2	45.7
Sparse Partial Weakly-Supervised	SPWOOD (ours)	44.1	45.7	46.3

390 Table 4: Detection accuracy
 391 under different combinations
 392 of weak annotations at the
 393 sparse-partial ratio 20-20.

RBox:HBox:Point	mAP
1:1:1	53.0
1:1:0	56.3
1:0:1	52.3
0:1:1	47.6
0:1:4	41.2

Table 5: mAP results of
 Sparse Annotation Learning
 with different weights under
 sparse-partial 20-20 ratio.

Weight	mAP
0.4	57.8
0.3	57.5
0.2	60.6
0.1	58.0

Table 6: Comparison of mAP
 performance across Sparse
 Annotation Learning (SAL)
 module in our framework
 in DOTA1.0 test set under
 sparse-partial 20-20 ratio.

Setting	mAP
with SAL	47.6
without SAL	42.0

4 EXPERIMENT

4.1 DATASET AND SETUP

To evaluate our proposed SPWOOD models, we conducted experiments on DOTA-v1.0/-v1.5 (Xia et al., 2018) and DIOR (Li et al., 2020). DOTA-v1.0 comprises 2,806 aerial images, consisting of 1,411 training images, 458 validation images, and 937 test images. The training and validation sets contain 188,282 instances across 15 categories. DOTA-v1.5 uses the same images as DOTA-v1.0 but features more annotations, with 403,318 instances across 16 categories, including a higher number of smaller objects. **The DIOR dataset comprises 23,463 images across 20 distinct object categories. The dataset is partitioned into 11,725 images for training and 11,738 images for testing.**

Taking the DOTA-V1.0 dataset as a representative example, to create sparse-partial weak supervision dataset, we select 10%, 20%, and 30% of the images as initial labeled data from the DOTA-v1.0 train-val set, while the remaining images are treated as unlabeled. From the labeled subset, we generate datasets using two distinct sparse methods. The first is the Single Sparse Method (Lu et al., 2024; Lin et al., 2025), which applies a specific sparse ratio (*i.e.* 10%, 20%, 30%) to each category within each image, keeping at least one annotation for any category present in the image. In contrast, our proposed Overall Sparse Method treats all labeled annotations as a unified group and samples annotations for each category at the desired ratio (*i.e.* 10%, 20%, 30%). For a fair comparison with prior studies, we conduct main experiments on the datasets generated by the Single Sparse Method, unless otherwise noted. Then we create the weakly-annotated data for training by simply omitting the orientation and scale information from the annotations. In our naming convention, we combine the partial-ratio and sparse-ratio (*i.e.* 30-10), where 30% indicates the partial-ratio and 10% indicates the sparse-ratio. Besides, all reported detection results of models are obtained by testing on test set.

Our proposed SPWOOD model is implemented using the MMRotate (Zhou et al., 2022) frameworks. We employ an FCOS detector (Tian et al., 2019) with a ResNet50 backbone (He et al., 2016) and a FPN (Lin et al., 2017) neck. The AdamW optimizer (Loshchilov & Hutter, 2017) is used for optimization. The entire training schedule consists of 180,000 iterations, which includes an initial burn-in stage of 12,800 iterations to stabilize model convergence in the early stage.

4.2 MAIN RESULT

DOTA-v1.0: We employ a simplified version of RSST, comprising both supervised and unsupervised branches, as our SAOD baseline, which we term RSST*. As summarized in Table 1, we present the

432
433 Table 7: Detection accuracy at sparse-
434 partial ratio 20-50 (RBox supervised).

Algorithm Types	Methods	20-50
Semi-Supervised	MCL	53.2
	PWOOD	59.8
Sparsely Supervised	S ² Teacher	56.5
	RSST	56.1
	RSST*	55.1
Sparse Partial Weakly-Supervised	SPWOOD (ours)	63.0

435
436 Table 8: The performance comparisons of our proposed
437 PWOOD framework based on different Pseudo-labels
438 Filtering Methods at different parse-partial ratios under
439 DOTA-v1.0 Dataset-Sparse-Partial setting.

Module	Methods	10-10	10-20	20-10	20-20
SPWOOD	w/ CPF	44.4	53.0	51.9	57.1
	w/ MPF	49.5	54.0	54.9	57.8

442 Table 9: Performance of the PWOOD Framework with Overall and Single Sparse Methods.

Algorithm paradigms	Methods	10-10	10-20	20-10	20-20	30-10	30-20
SPWOOD	Overall Sparse Method	41.7	49.1	47.9	57.2	52.3	57.5
	Single Sparse Method	49.5	54.0	54.9	57.8	54.9	60.3

448 detection results of different methods on DOTA-v1.0 dataset and SPWOOD exhibits a substantial
449 and consistent improvement over other methods across all sparse-partial ratios. Notably, SPWOOD
450 achieves superior performance using the less-informative HBox annotations, even outperforming
451 the RSST* model that utilizes corresponding proportions of RBox annotations with gains of 3.1%
452 (10-10), 6.4% (10-20), 10.5% (20-10) and 3.0% (20-20). It means that SPWOOD delivers excellent
453 performance at a lower cost. The effectiveness of SPWOOD under weak supervision is further high-
454 lighted by comparisons with WOOD methods. Compared to H2RBox-v2, SPWOOD achieves large
455 margins of improvement, yielding gains of 14.9% (10-10), 21.1% (10-20), 13.7% (20-10), 11.3%
456 (20-20), 9.2% (30-10), and 7.3% (30-20) under the corresponding HBox annotations. Similarly,
457 under point annotations, SPWOOD improves mAP by 17.9%, 27.0%, 19.1%, 15.6%, 20.7%, and
458 14.8%, respectively, compared to Point2RBox-v2. These results strongly underscore SPWOOD’s
459 excellent capability in the sparse-partial, weakly-supervised oriented object detection task.

460 Concurrently, SPWOOD’s ability to support multiple annotation formats within a unified framework
461 offers a highly effective paradigm for reducing the data acquisition burden. As detailed in Table 1
462 (*i.e.* R:H:P=1:1:1), we conducted experiments to evaluate the framework’s performance under di-
463 verse labeling scenarios, using a combination of Point, HBox, and RBox annotations as input. The
464 detection performance significantly surpasses WOOD and SOOD methods. Crucially, SPWOOD
465 achieves highly competitive performance compared to the current State-of-the-Art SAOD methods
466 across different sparse-partial ratios. [In Table 4, we present comprehensive results from experiments](#)
467 [conducted under different mixed weak annotation settings. This analysis empirically confirms the](#)
468 [robust capability of our framework to accommodate and leverage different types of weak supervi-](#)
469 [sion concurrently.](#) Furthermore, as detailed in Table 7, we present the results at the ratio 20-50,
470 highlighting SPWOOD’s effectiveness in utilizing limited annotation resources.

471 More Results: As shown in Table 2, to provide additional validation for our proposed framework’s
472 efficacy, we performed a thorough comparative analysis under RBox annotations on DOTA-v1.5
473 dataset. Our proposed SPWOOD outperforms RSST* with gains of 7% (10-10), 12.1% (10-20),
474 6.7% (20-10), 6.1% (20-20), 5.6% (30-10) and 3.3% (30-20), respectively. Compared to the gain on
475 DOTA-v1.0 (6.1%, 8.5%, 13.2%, 6.8%, 1.7%, and 3.8%, respectively), SPWOOD’s performance
476 on DOTA-v1.5 highlights its robustness and adaptability in complex scenes with smaller objects. [To](#)
477 [validate the capability of our model across different datasets, we conducted additional experiments](#)
478 [on the DIOR dataset. As demonstrated in Table 3, our model consistently outperforms all competing](#)
479 [methods across all the ratios.](#)

480 4.3 ABLATION STUDIES
481

482 The selection of pseudo-labels directly impacts the model’s subsequent training, making the filtering
483 strategy crucial. As detailed in Table 8, we conducted a rigorous systematic evaluation of our pro-
484 posed Multi-level Pseudo-label Filtering (MPF) algorithm against the Class-Agnostic Pseudo-label
485 Filtering (CPF) approach (Liu et al., 2025a). Our MPF method consistently outperforms CPF across
486 all tested sparse-partial ratios on the DOTA-v1.0 dataset. Specifically, our MPF method achieves

486
 487 Table 10: Annotation Statistics and Performance Analysis for Overall and Single Sparse Methods
 488 at sparse-partial ratio 10-10, 20-10 and 30-10. Δ and ∇ mean annotations numbers under Single and
 489 Overall Sparse Method. \blacksquare presents relative difference among corresponding numbers.

Category	PL	BD	BR	GTF	SV	LV	SH	TC	BC	ST	SBF	RA	HA	SP	HC
Annotation at 30-10	762 Δ	88	211	242	2083	1342	2344	238	81	376	137	156	514	225	40
	785 ∇	37	114	39	2163	1319	2316	189	44	389	34	40	567	124	25
Relative Difference	-2.9% \blacksquare	+137.8	+85.1	+520.5	-3.7	+1.7	+1.2	+25.9	+84.1	-3.3	+302.9	+290.0	-9.3	+81.5	+60.0
Annotation at 20-10	551 Δ	57	117	151	1256	863	1868	180	59	306	90	99	352	157	40
	585 ∇	19	68	24	1270	873	1824	121	35	275	22	27	366	111	30
Relative Difference	-5.8% \blacksquare	+200	+72.1	+529.2	-1.1	-1.1	+2.4	+48.8	+68.6	+11.3	+309.1	+266.7	-3.8	+41.4	+33.3
Annotation at 10-10	383 Δ	37	77	79	767	479	846	100	25	224	48	46	134	110	32
	369 ∇	14	29	13	779	491	870	78	20	232	12	11	145	95	24
Relative Difference	+3.8% \blacksquare	+164.3	+165.5	+507.7	-1.5	-2.4	-2.8	+28.2	+25.0	-3.4	+300	+318.2	-7.6	+15.8	+33.3
AP at 10-10	71.6 Δ	46.8	17.3	53.6	55.0	52.3	73.2	86.1	50.3	62.5	27.6	48.1	19.8	53.9	23.0
	73.4 ∇	23.6	17.6	25.6	55.9	56.4	72.6	88.8	37.1	67.5	0.40	24.8	18.5	40.8	18.0
Relative Difference	-2.5% \blacksquare	+98.6	-1.7	+109.4	-1.6	-7.2	+0.8	-3.1	+35.5	-7.5	+583.0	+94.2	+6.9	+32.1	+27.6

502 notable mAP improvements of 5.1% (10-10), 1.0% (10-20), 3.0% (20-10), and 0.7% (20-20), re-
 503 spectively. The most significant gains are observed at lower annotation sparsity levels (e.g., 10-10),
 504 demonstrating MPF’s superior capability in extremely sparse settings. This superior performance
 505 stems from MPF’s ability to effectively capture intricate relationships within the model’s multi-level
 506 predictions, thereby achieving superior detection accuracy even with limited supervision.

507 **Sparse Processing Method Analysis:** To rigorously evaluate the impact of data generation on model
 508 performance, we conducted ablation study focusing on datasets created by two sparse methods.
 509 As shown in Table 9, the SPWOOD model demonstrates consistently superior performance on the
 510 dataset derived from Single Sparse Method compared to Overall Sparse Method, with gains of 7.8%,
 511 4.9%, 7.0%, 0.6%, 2.6%, and 2.8% across the corresponding ratios. As detailed in Table 10, the Sin-
 512 ggle Sparse Method tends to retain more annotations for categories with initially scarce labels, such
 513 as baseball diamond, ground track field, soccer-ball field, and roundabout. We further analyzed
 514 the direct relationship between annotation count and detection accuracy (Table 10). For instance,
 515 considering the baseball-diamond category under ratio 10-10, the Single Sparse Method yielded a
 516 164.3% relative increase in annotation count compared to the Overall Sparse Method. This sub-
 517 stantial data advantage directly translated into a near 100% (98.6%) relative difference on AP per-
 518 formance. These findings decisively reveal that relatively higher annotation count leads to superior
 519 detection accuracy, which is particularly pronounced for categories with few initial annotations.

520 **More results:** We conducted an ablation study on the parameter w within our Sparse Annotation
 521 Learning module, as shown in Table 5. In our framework, the primary function of w is to suppress
 522 the influence of hard negatives, ensuring robust training despite sparse annotations. Furthermore, we
 523 performed a ablation study about Sparse Annotation Learning module in the SOS-Student compo-
 524 nent, with results presented in Table 6. The substantial performance degradation observed after
 525 removing this module clearly underscores its critical contribution in the sparse setting. These results
 526 underscore the Sparse Annotation Learning module’s efficacy in semi-sparse setting.

5 CONCLUSION

527 In this work, we propose a Sparse Partial Weakly-Supervised Oriented Object Detection (SPWOOD)
 528 framework, which leverages the strengths of mainstream oriented object detection methods to sig-
 529 nificantly reduce the need for annotation in remote sensing. Given the sparse weak annotation data,
 530 we introduce three core components—sparse annotation learning, orientation learning, and scale
 531 learning—to form SOS-Student model. To effectively utilize abundant unlabeled data, we employ
 532 a Multi-level Pseudo-labels Filtering mechanism to select reliable supervised signals. Extensive ex-
 533 periments on benchmark datasets demonstrate that SPWOOD outperforms existing OOD methods,
 534 all with a minimal annotation cost. Furthermore, we introduce an novel sparse processing method,
 535 guaranteeing that the sparse dataset maintains the same distribution as the original data. **One cur-
 536 rent limitation of our approach is that it exclusively utilizes a single visual modality.** Incorporating
 537 additional data modalities (e.g., spectral or textual information) is posited as an interesting future
 538 research direction, particularly for further improving performance within sparse annotation settings.

540
541
ETHICS STATEMENT542
543
544
545
This work is conducted in accordance with all ethical standards. We have appropriately cited all
compared and referenced methods. The datasets used are publicly available and have been appropriately
cited. We have ensured that our data collection and processing methods, as well as the release
of our code, do not violate privacy rights or intellectual property laws.546
547
REPRODUCIBILITY STATEMENT
548549
550
551
552
553
To ensure the reproducibility of our work, we have provided comprehensive details of our experimental
setup, methodology, and results. This includes a clear description of the algorithms, model
architectures, hyperparameters, and training procedures used. We will make our source code, including
all necessary scripts and configurations, publicly available upon publication. Besides, we will provide
detailed instructions on how to prepare sparse partial weak supervision dataset.554
555
REFERENCES
556557
558
Franz Aurenhammer. Voronoi diagrams—a survey of a fundamental geometric data structure. *ACM computing surveys (CSUR)*, 23(3):345–405, 1991.
559
560
Hakan Bilen, Marco Pedersoli, and Tinne Tuytelaars. Weakly supervised object detection with
convex clustering. In *Proceedings of the IEEE conference on computer vision and pattern recognition*, pp. 1081–1089, 2015.
561
562
563
Guangming Cao, Xuehui Yu, Wenwen Yu, Xumeng Han, Xue Yang, Guorong Li, Jianbin Jiao,
and Zhenjun Han. P2rbox: Point prompt oriented object detection with sam. *arXiv preprint arXiv:2311.13128*, 2023.
564
565
566
Binghui Chen, Pengyu Li, Xiang Chen, Biao Wang, Lei Zhang, and Xian-Sheng Hua. Dense learning
based semi-supervised object detection. In *Proceedings of the IEEE/CVF conference on computer vision and pattern recognition*, pp. 4815–4824, 2022a.
567
568
569
Liangyu Chen, Tong Yang, Xiangyu Zhang, Wei Zhang, and Jian Sun. Points as queries: Weakly
semi-supervised object detection by points. In *Proceedings of the IEEE/CVF conference on computer vision and pattern recognition*, pp. 8823–8832, 2021.
570
571
572
573
Pengfei Chen, Xuehui Yu, Xumeng Han, Najmul Hassan, Kai Wang, Jiachen Li, Jian Zhao,
Humphrey Shi, Zhenjun Han, and Qixiang Ye. Point-to-box network for accurate object detection
via single point supervision. In *European Conference on Computer Vision*, pp. 51–67. Springer,
2022b.
574
575
576
577
Jian Ding, Nan Xue, Yang Long, Gui-Song Xia, and Qikai Lu. Learning roi transformer for oriented
object detection in aerial images. In *Proceedings of the IEEE/CVF conference on computer vision and pattern recognition*, pp. 2849–2858, 2019.
578
579
580
Kaiming He, Xiangyu Zhang, Shaoqing Ren, and Jian Sun. Deep residual learning for image recognition.
In *Proceedings of the IEEE conference on computer vision and pattern recognition*, pp. 770–778, 2016.
581
582
583
584
Shitian He, Huanxin Zou, Yingqian Wang, Boyang Li, Xu Cao, and Ning Jing. Learning remote
sensing object detection with single point supervision. *IEEE Transactions on Geoscience and Remote Sensing*, 62:1–16, 2023.
585
586
587
Wei Hua, Dingkang Liang, Jingyu Li, Xiaolong Liu, Zhikang Zou, Xiaoqing Ye, and Xiang Bai.
Sood: Towards semi-supervised oriented object detection. In *Proceedings of the IEEE/CVF conference on computer vision and pattern recognition*, pp. 15558–15567, 2023.
588
589
590
591
Javed Iqbal, Muhammad Akhtar Munir, Arif Mahmood, Afsheen Rafaqat Ali, and Mohsen Ali.
Leveraging orientation for weakly supervised object detection with application to firearm localization.
Neurocomputing, 440:310–320, 2021.

594 Alexander Kirillov, Eric Mintun, Nikhila Ravi, Hanzi Mao, Chloe Rolland, Laura Gustafson, Tete
 595 Xiao, Spencer Whitehead, Alexander C Berg, Wan-Yen Lo, et al. Segment anything. In *Proceedings of the IEEE/CVF international conference on computer vision*, pp. 4015–4026, 2023.
 596

598 Gang Li, Xiang Li, Yujie Wang, Yichao Wu, Ding Liang, and Shanshan Zhang. Pseco: Pseudo
 599 labeling and consistency training for semi-supervised object detection. In *European Conference
 600 on Computer Vision*, pp. 457–472. Springer, 2022a.

601 Hengduo Li, Zuxuan Wu, Abhinav Shrivastava, and Larry S Davis. Rethinking pseudo labels for
 602 semi-supervised object detection. In *Proceedings of the AAAI conference on artificial intelligence*,
 603 volume 36, pp. 1314–1322, 2022b.

604 Ke Li, Gang Wan, Gong Cheng, Liqui Meng, and Junwei Han. Object detection in optical remote
 605 sensing images: A survey and a new benchmark. *ISPRS journal of photogrammetry and remote
 606 sensing*, 159:296–307, 2020.

608 Wentong Li, Wenyu Liu, Jianke Zhu, Miaomiao Cui, Xian-Sheng Hua, and Lei Zhang. Box-
 609 supervised instance segmentation with level set evolution. In *European conference on computer
 610 vision*, pp. 1–18. Springer, 2022c.

612 Dingkang Liang, Wei Hua, Chunsheng Shi, Zhikang Zou, Xiaoqing Ye, and Xiang Bai. Sood++:
 613 Leveraging unlabeled data to boost oriented object detection. *arXiv preprint arXiv:2407.01016*,
 614 2024.

615 Wei Liao, Chunyan Xu, Chenxu Wang, and Zhen Cui. Llm-assisted semantic guidance for sparsely
 616 annotated remote sensing object detection. *arXiv preprint arXiv:2509.16970*, 2025.

618 Tsung-Yi Lin, Piotr Dollár, Ross Girshick, Kaiming He, Bharath Hariharan, and Serge Belongie.
 619 Feature pyramid networks for object detection. In *Proceedings of the IEEE conference on com-
 620 puter vision and pattern recognition*, pp. 2117–2125, 2017.

621 Yu Lin, Jianghang Lin, Kai Ye, You Shen, Yan Zhang, Shengchuan Zhang, Liujuan Cao, and Ron-
 622 grong Ji. S 2 teacher: Step-by-step teacher for sparsely annotated oriented object detection. *arXiv
 623 preprint arXiv:2504.11111*, 2025.

625 Liang Liu, Boshen Zhang, Jiangning Zhang, Wuhao Zhang, Zhenye Gan, Guanzhong Tian, Wenbing
 626 Zhu, Yabiao Wang, and Chengjie Wang. Mixteacher: Mining promising labels with mixed scale
 627 teacher for semi-supervised object detection. In *Proceedings of the IEEE/CVF conference on
 628 computer vision and pattern recognition*, pp. 7370–7379, 2023.

629 Mingxin Liu, Peiyuan Zhang, Yuan Liu, Wei Zhang, Yue Zhou, Ning Liao, Ziyang Gong, Junwei
 630 Luo, Zhirui Wang, Yi Yu, et al. Partial weakly-supervised oriented object detection. *arXiv preprint
 631 arXiv:2507.02751*, 2025a.

633 Nanqing Liu, Xun Xu, Yongyi Su, Haojie Zhang, and Heng-Chao Li. Pointsam: Pointly-supervised
 634 segment anything model for remote sensing images. *IEEE Transactions on Geoscience and Re-
 635 mote Sensing*, 2025b.

636 Yen-Cheng Liu, Chih-Yao Ma, Zijian He, Chia-Wen Kuo, Kan Chen, Peizhao Zhang, Bichen Wu,
 637 Zsolt Kira, and Peter Vajda. Unbiased teacher for semi-supervised object detection. *arXiv preprint
 638 arXiv:2102.09480*, 2021.

640 Yen-Cheng Liu, Chih-Yao Ma, and Zsolt Kira. Unbiased teacher v2: Semi-supervised object detec-
 641 tion for anchor-free and anchor-based detectors. In *Proceedings of the IEEE/CVF Conference on
 642 Computer Vision and Pattern Recognition*, pp. 9819–9828, 2022.

643 Ilya Loshchilov and Frank Hutter. Decoupled weight decay regularization. *arXiv preprint
 644 arXiv:1711.05101*, 2017.

646 Zihan Lu, Chenxu Wang, Chunyan Xu, Xiangwei Zheng, and Zhen Cui. Progressive explora-
 647 tion-conformal learning for sparsely annotated object detection in aerial images. *Advances in Neural
 648 Information Processing Systems*, 37:40593–40614, 2024.

648 Junwei Luo, Xue Yang, Yi Yu, Qingyun Li, Junchi Yan, and Yansheng Li. Pointobb: Learning
 649 oriented object detection via single point supervision. In *Proceedings of the IEEE/CVF conference*
 650 *on computer vision and pattern recognition*, pp. 16730–16740, 2024.

651 Yuxiang Nie, Chaowei Fang, Lechao Cheng, Liang Lin, and Guanbin Li. Adapting object size
 652 variance and class imbalance for semi-supervised object detection. In *Proceedings of the AAAI*
 653 *Conference on Artificial Intelligence*, volume 37, pp. 1966–1974, 2023.

654 Sai Saketh Rambhatla, Saksham Suri, Rama Chellappa, and Abhinav Shrivastava. Sparsely
 655 annotated object detection: A region-based semi-supervised approach. *arXiv preprint*
 656 *arXiv:2201.04620*, 7, 2022.

657 Botao Ren, Xue Yang, Yi Yu, Junwei Luo, and Zhidong Deng. Pointobb-v2: Towards simpler, faster,
 658 and stronger single point supervised oriented object detection. *arXiv preprint arXiv:2410.08210*,
 659 2024.

660 Peize Sun, Yi Jiang, Enze Xie, Wenqi Shao, Zehuan Yuan, Changhu Wang, and Ping Luo. What
 661 makes for end-to-end object detection? In *International Conference on Machine Learning*, pp.
 662 9934–9944. PMLR, 2021a.

663 Yongqing Sun, Jie Ran, Feng Yang, Chenqiang Gao, Takayuki Kurozumi, Hideaki Kimata, and Ziqi
 664 Ye. Oriented object detection for remote sensing images based on weakly supervised learning.
 665 In *2021 IEEE International Conference on Multimedia & Expo Workshops (ICMEW)*, pp. 1–6.
 666 IEEE, 2021b.

667 Saksham Suri, Saketh Rambhatla, Rama Chellappa, and Abhinav Shrivastava. Sparsedet: Improving
 668 sparsely annotated object detection with pseudo-positive mining. In *Proceedings of the IEEE/CVF*
 669 *International Conference on Computer Vision*, pp. 6770–6781, 2023.

670 Antti Tarvainen and Harri Valpola. Mean teachers are better role models: Weight-averaged con-
 671 sistency targets improve semi-supervised deep learning results. *Advances in neural information*
 672 *processing systems*, 30, 2017.

673 Zhi Tian, Chunhua Shen, Hao Chen, and Tong He. Fcos: Fully convolutional one-stage object
 674 detection. In *Proceedings of the IEEE/CVF international conference on computer vision*, pp.
 675 9627–9636, 2019.

676 Zhi Tian, Chunhua Shen, Xinlong Wang, and Hao Chen. Boxinst: High-performance instance
 677 segmentation with box annotations. In *Proceedings of the IEEE/CVF conference on computer*
 678 *vision and pattern recognition*, pp. 5443–5452, 2021.

679 Luc Vincent and Pierre Soille. Watersheds in digital spaces: an efficient algorithm based on im-
 680 mersion simulations. *IEEE Transactions on Pattern Analysis & Machine Intelligence*, 13(06):
 681 583–598, 1991.

682 Chenxu Wang, Chunyan Xu, Xiang Li, YuXuan Li, Xu Guo, Ziqi Gu, and Zhen Cui. Multi-clue
 683 consistency learning to bridge gaps between general and oriented object in semi-supervised detec-
 684 tion. In *Proceedings of the AAAI Conference on Artificial Intelligence*, volume 39, pp. 7582–7590,
 685 2025.

686 Haohan Wang, Liang Liu, Boshen Zhang, Jiangning Zhang, Wuhao Zhang, Zhenye Gan, Yabiao
 687 Wang, Chengjie Wang, and Haoqian Wang. Calibrated teacher for sparsely annotated object
 688 detection. In *Proceedings of the AAAI Conference on Artificial Intelligence*, volume 37, pp.
 689 2519–2527, 2023a.

690 Linfei Wang, Yibing Zhan, Xu Lin, Baosheng Yu, Liang Ding, Jianqing Zhu, and Dapeng Tao.
 691 Explicit and implicit box equivariance learning for weakly-supervised rotated object detection.
 692 *IEEE Transactions on Emerging Topics in Computational Intelligence*, 9(1):509–521, 2024.

693 Tiancai Wang, Tong Yang, Jiale Cao, and Xiangyu Zhang. Co-mining: Self-supervised learning for
 694 sparsely annotated object detection. In *Proceedings of the AAAI conference on artificial intelli-
 695 gence*, volume 35, pp. 2800–2808, 2021.

702 Xinjiang Wang, Xingyi Yang, Shilong Zhang, Yijiang Li, Litong Feng, Shijie Fang, Chengqi Lyu,
 703 Kai Chen, and Wayne Zhang. Consistent-teacher: Towards reducing inconsistent pseudo-targets
 704 in semi-supervised object detection. In *Proceedings of the IEEE/CVF conference on computer*
 705 *vision and pattern recognition*, pp. 3240–3249, 2023b.

706 Yidong Wang, Hao Chen, Qiang Heng, Wenxin Hou, Yue Fan, Zhen Wu, Jindong Wang, Marios
 707 Savvides, Takahiro Shinozaki, Bhiksha Raj, et al. Freematch: Self-adaptive thresholding for
 708 semi-supervised learning. *arXiv preprint arXiv:2205.07246*, 2022.

710 Gui-Song Xia, Xiang Bai, Jian Ding, Zhen Zhu, Serge Belongie, Jiebo Luo, Mihai Datcu, Marcello
 711 Pelillo, and Liangpei Zhang. Dota: A large-scale dataset for object detection in aerial images. In
 712 *Proceedings of the IEEE conference on computer vision and pattern recognition*, pp. 3974–3983,
 713 2018.

714 Qiming Xia, Jinhao Deng, Chenglu Wen, Hai Wu, Shaoshuai Shi, Xin Li, and Cheng Wang. Coin:
 715 Contrastive instance feature mining for outdoor 3d object detection with very limited annotations.
 716 In *Proceedings of the IEEE/CVF International Conference on Computer Vision*, pp. 6254–6263,
 717 2023.

719 Qiming Xia, Wei Ye, Hai Wu, Shijia Zhao, Leyuan Xing, Xun Huang, Jinhao Deng, Xin Li, Chenglu
 720 Wen, and Cheng Wang. Hinted: Hard instance enhanced detector with mixed-density feature
 721 fusion for sparsely-supervised 3d object detection. In *Proceedings of the IEEE/CVF Conference*
 722 *on Computer Vision and Pattern Recognition*, pp. 15321–15330, 2024.

724 Xingxing Xie, Gong Cheng, Jiabao Wang, Xiwen Yao, and Junwei Han. Oriented r-cnn for object
 725 detection. In *Proceedings of the IEEE/CVF international conference on computer vision*, pp.
 726 3520–3529, 2021.

727 Ke Yang, Dongsheng Li, and Yong Dou. Towards precise end-to-end weakly supervised object
 728 detection network. In *Proceedings of the IEEE/CVF international conference on computer vision*,
 729 pp. 8372–8381, 2019a.

731 Xue Yang, Jirui Yang, Junchi Yan, Yue Zhang, Tengfei Zhang, Zhi Guo, Xian Sun, and Kun Fu.
 732 Scrdet: Towards more robust detection for small, cluttered and rotated objects. In *Proceedings of*
 733 *the IEEE/CVF international conference on computer vision*, pp. 8232–8241, 2019b.

734 Xue Yang, Junchi Yan, Ziming Feng, and Tao He. R3det: Refined single-stage detector with feature
 735 refinement for rotating object. In *Proceedings of the AAAI conference on artificial intelligence*,
 736 volume 35, pp. 3163–3171, 2021.

738 Xue Yang, Gefan Zhang, Xiaojiang Yang, Yue Zhou, Wentao Wang, Jin Tang, Tao He, and Junchi
 739 Yan. Detecting rotated objects as gaussian distributions and its 3-d generalization. *IEEE Trans-*
 740 *actions on Pattern Analysis and Machine Intelligence*, 45(4):4335–4354, 2022.

741 Xue Yang, Gefan Zhang, Wentong Li, Xuehui Wang, Yue Zhou, and Junchi Yan. H2rbox: Horizontal
 742 box annotation is all you need for oriented object detection. *International Conference on Learning*
 743 *Representations*, 2023.

745 Xinyi Ying, Li Liu, Yingqian Wang, Ruojing Li, Nuo Chen, Zaiping Lin, Weidong Sheng, and Shilin
 746 Zhou. Mapping degeneration meets label evolution: Learning infrared small target detection with
 747 single point supervision. In *Proceedings of the IEEE/CVF conference on computer vision and*
 748 *pattern recognition*, pp. 15528–15538, 2023.

749 Yi Yu, Xue Yang, Qingyun Li, Yue Zhou, Feipeng Da, and Junchi Yan. H2rbox-v2: Incorporating
 750 symmetry for boosting horizontal box supervised oriented object detection. *Advances in Neural*
 751 *Information Processing Systems*, 36:59137–59150, 2023.

753 Yi Yu, Xue Yang, Qingyun Li, Feipeng Da, Jifeng Dai, Yu Qiao, and Junchi Yan. Point2rbox:
 754 Combine knowledge from synthetic visual patterns for end-to-end oriented object detection with
 755 single point supervision. In *Proceedings of the IEEE/CVF conference on computer vision and*
 756 *pattern recognition*, pp. 16783–16793, 2024.

756 Yi Yu, Botao Ren, Peiyuan Zhang, Mingxin Liu, Junwei Luo, Shaofeng Zhang, Feipeng Da, Junchi
757 Yan, and Xue Yang. Point2rbox-v2: Rethinking point-supervised oriented object detection with
758 spatial layout among instances. In *Proceedings of the Computer Vision and Pattern Recognition*
759 *Conference*, pp. 19283–19293, 2025a.

760 Yi Yu, Xue Yang, Yansheng Li, Zhenjun Han, Feipeng Da, and Junchi Yan. Wholly-wood: Wholly
761 leveraging diversified-quality labels for weakly-supervised oriented object detection. *IEEE Trans-*
762 *actions on Pattern Analysis and Machine Intelligence*, 2025b.

763 Dingwen Zhang, Junwei Han, Gong Cheng, and Ming-Hsuan Yang. Weakly supervised object local-
764 *ization and detection: A survey. IEEE transactions on pattern analysis and machine intelligence*,
765 44(9):5866–5885, 2021.

766 Peiyuan Zhang, Junwei Luo, Xue Yang, Yi Yu, Qingyun Li, Yue Zhou, Xiaosong Jia, Xudong Lu,
767 Jingdong Chen, Xiang Li, et al. Pointobb-v3: Expanding performance boundaries of single point-
768 supervised oriented object detection. *International Journal of Computer Vision*, pp. 1–21, 2025.

769 Like Zhao, Shunyi Zheng, Wenjing Yang, Haitao Wei, and Xia Huang. An image thresholding
770 approach based on gaussian mixture model. *Pattern Analysis and Applications*, 22(1):75–88,
771 2019.

772 Yuanyi Zhong, Jianfeng Wang, Jian Peng, and Lei Zhang. Boosting weakly supervised object de-
773 tection with progressive knowledge transfer. In *European conference on computer vision*, pp.
774 615–631. Springer, 2020.

775 Yue Zhou, Xue Yang, Gefan Zhang, Jiabao Wang, Yanyi Liu, Liping Hou, Xue Jiang, Xingzhao Liu,
776 Junchi Yan, Chengqi Lyu, et al. Mmrotate: A rotated object detection benchmark using pytorch.
777 In *Proceedings of the 30th ACM International Conference on Multimedia*, pp. 7331–7334, 2022.

778 Tianyu Zhu, Bryce Ferenczi, Pulak Purkait, Tom Drummond, Hamid Rezatofighi, and Anton Van
779 Den Hengel. Knowledge combination to learn rotated detection without rotated annotation. In
780 *Proceedings of the IEEE/CVF Conference on Computer Vision and Pattern Recognition*, pp.
781 15518–15527, 2023.

782

783

784

785

786

787

788

789

790

791

792

793

794

795

796

797

798

799

800

801

802

803

804

805

806

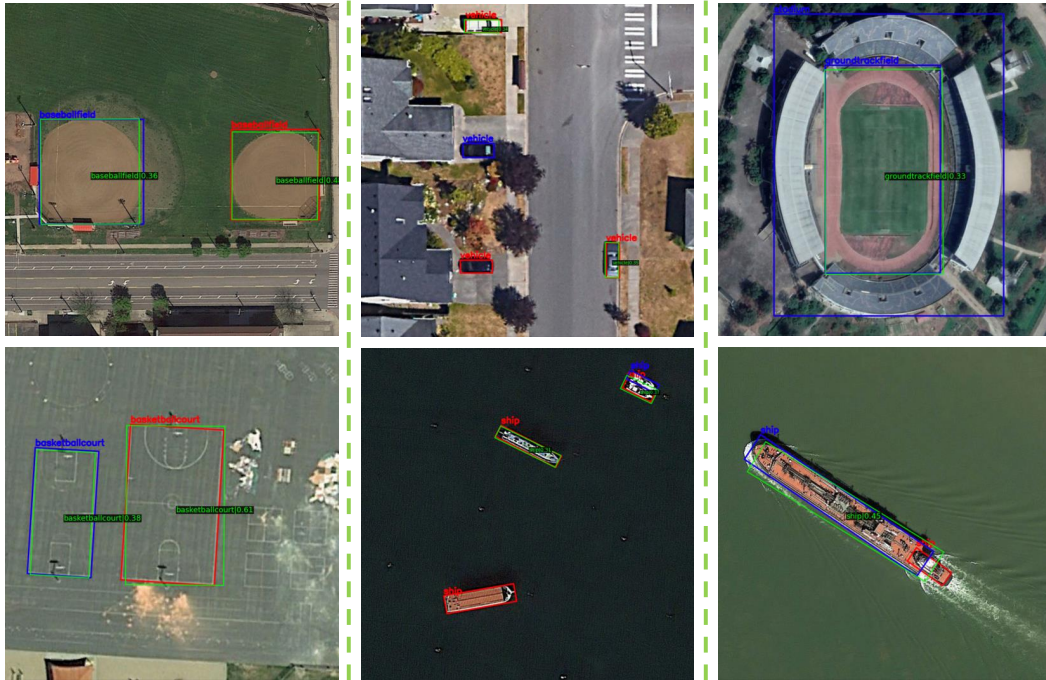
807

808

809

810
811 Table 11: Comparison of computational costs across different methods for the OOD task on DIOR
812 test set under different sparse-partial ratios (RBox supervised).

813 814 Algorithm Types	815 Methods	816 memory usage	817 running time
815 Semi-Supervised	816 MCL	817 5598MB	818 16hours
816 Partial Weakly-Supervised	817 PWOOD	818 9021MB	819 23hours
817 Sparsely Supervised	818 RSST	819 13672MB	820 34hours
818 Sparse Partial 819 Weakly-Supervised	820 SPWOOD (ours)	821 22785MB	822 40hours



823
824 Figure 3: Qualitative results showing the qualities of the detection performance.
825
826
827
828
829
830
831
832
833

834 A APPENDIX

835 A.1 THE USE OF LARGE LANGUAGE MODELS (LLMS)

836 We affirm that this paper is prepared and written entirely by us. We did not use any large language
837 models (LLMs) to generate the abstract, content, or any part of the text. The ideas, analysis, and
838 conclusions presented are the sole product of the authors' original thought and research. We did,
839 however, utilize standard tools like grammar checkers for minor stylistic improvements.

840 A.2 COMPUTATIONAL COST COMPARISON

841 As shown in Table 11, the operational cost (time and computational resource consumption) of our
842 spwood method is observed to be higher compared to other models. This increase is primarily
843 attributed to two factors: The necessary overhead associated with processing multiple weak
844 annotations within the model, like combination of HBox and point. The substantial computational load
845 required for effectively handling the highly sparse annotation settings, where extensive calculations
846 are performed to compensate for the lack of dense supervision.

864
865

A.3 FAILURE ANALYSIS

866 As depicted in Figure 3, we use different colors to illustrate the different bounding boxes under
867 sparse conditions: the blue boxes represent the sparse annotations used for training; the red boxes
868 indicate objects that were omitted from the labels due to the sparse setting; and the green boxes
869 represent the final objects detected by our SPWOOD framework. The figure highlights the following
870 scenarios and challenges:

871 Column 1 (Effectiveness in Sparse Setting): This column demonstrates our model’s effectiveness in
872 sparse scenarios, showing its ability to learn class features from partially labeled data and success-
873 fully detect other unlabeled instances of the same category in image.

874 Column 2 (Intra-class Variance Challenge): This column highlights cases where the model fails to
875 detect certain objects. This failure is typically due to significant intra-class variance (differences
876 within the same category) present in the sparsely annotated data.

877 Column 3 (Complex Spatial Arrangement Challenge): This section illustrates the performance
878 degradation observed when dealing with complex spatial arrangements, such such as large objects
879 containing smaller ones or closely packed, overlapping instances.

880

881

882

883

884

885

886

887

888

889

890

891

892

893

894

895

896

897

898

899

900

901

902

903

904

905

906

907

908

909

910

911

912

913

914

915

916

917